Journal of Visualized Experiments

Controlled Semi-Automated Lased-Induced Injuries for Studying Spinal Cord Regeneration in Zebrafish Larvae

--Manuscript Draft--

Article Type:	Invited Methods Collection - JoVE Produced Video
Manuscript Number:	JoVE63259R2
Full Title:	Controlled Semi-Automated Lased-Induced Injuries for Studying Spinal Cord Regeneration in Zebrafish Larvae
Corresponding Author:	Francois El-Daher The University of Edinburgh Centre for Discovery Brain Sciences Edinburgh, Midlothian UNITED KINGDOM
Corresponding Author's Institution:	The University of Edinburgh Centre for Discovery Brain Sciences
Corresponding Author E-Mail:	francois.el-daher@ed.ac.uk
Order of Authors:	Francois El-Daher
	Jason J. Early
	Claire E. Richmond
	Rory Jamieson
	Thomas Becker
	Catherina G. Becker
Additional Information:	
Question	**Response**
Please specify the section of the submitted manuscript.	Medicine
Please indicate whether this article will be Standard Access or Open Access.	Standard Access ($1400)
Please indicate the **city, state/province, and country** where this article will be **filmed**. Please do not use abbreviations.	Edinburgh, United Kingdom
Please confirm that you have read and agree to the terms and conditions of the author license agreement that applies below:	I agree to the UK Author License Agreement (for UK authors only)
Please confirm that you have read and agree to the terms and conditions of the video release that applies below:	I agree to the Video Release
Please provide any comments to the journal here.	Dear Editor, the script files will be uploaded in the following week to the GitHub repository. Thank you for your understanding. Best regards.

TITLE:

Controlled Semi-Automated Lased-Induced Injuries for Studying Spinal Cord Regeneration in Zebrafish Larvae

AUTHORS AND AFFILIATIONS:

Francois El-Daher[1]*, Jason J. Early[1], Claire E. Richmond[1], Rory Jamieson[1], Thomas Becker[1,2], Catherina G. Becker[1,2]

[1]Centre for Discovery Brain Sciences, University of Edinburgh Medical School: Biomedical Sciences, Edinburgh EH16 4SB, UK

[2]Center for Regenerative Therapies at the TU Dresden, Fetscherstraße 105, 01307 Dresden, Germany

Email addresses of the authors:

Francois El-Daher (francois.el-daher@ed.ac.uk)
Jason J. Early (Jason.Early@ed.ac.uk)
Claire E. Richmond (c.e.richmond@sms.ed.ac.uk)
Rory Jamieson (r.jamieson-7@sms.ed.ac.uk)
Thomas Becker (thomas.becker@tu-dresden.de)
Catherina G. Becker (catherina.becker@tu-dresden.de)

*Email address of the corresponding author:

Francois El-Daher (francois.el-daher@ed.ac.uk)

SUMMARY:

The present protocol describes a method to induce tissue-specific and highly reproducible injuries in zebrafish larvae using a laser lesion system combined with an automated microfluidic platform for larvae handling.

ABSTRACT:

Zebrafish larvae possess a fully functional central nervous system (CNS) with a high regenerative capacity only a few days after fertilization. This makes this animal model very useful for studying spinal cord injury and regeneration. The standard protocol for inducing such lesions is to transect the dorsal part of the trunk manually. However, this technique requires extensive training and damages additional tissues. A protocol was developed for laser-induced lesions to circumvent these limitations, allowing for high reproducibility and completeness of spinal cord transection over many animals and between different sessions, even for an untrained operator. Furthermore, tissue damage is mainly limited to the spinal cord itself, reducing confounding effects from injuring different tissues, e.g., skin, muscle, and CNS. Moreover, hemi-lesions of the spinal cord are possible. Improved preservation of tissue integrity after laser injury facilitates further dissections needed for additional analyses, such as electrophysiology. Hence, this method offers precise control of the injury extent that is unachievable manually. This allows for new experimental paradigms in this powerful model in the future.

INTRODUCTION:

In contrast to mammals, zebrafish (*Danio rerio*) can repair their central nervous system (CNS) after injury[1]. The use of zebrafish larvae as a model for spinal cord regeneration is relatively recent. It has proven valuable to investigate the cellular and molecular mechanisms underlying repair[2]. This is due to the ease of manipulation, the short experimental cycle (new larvae every week), the tissues' optical transparency, and the larvae's small size, ideally suited for *in vivo* fluorescence microscopy.

In the case of spinal cord regeneration, two additional advantages of using larvae are the speed of recovery, a few days compared to a few weeks for adults, and the ease of inducing injuries using manual techniques. This has been successfully used in many studies[3,4,5], including recent investigations[6,7]. Overall, this leads to increased meaningful data production, high adaptability of experimental protocols, and decreased experimental costs. The use of larvae younger than 5 days post-fertilization also reduces the use of animals following the 3R principles in animal research[8].

After a spinal cord injury in zebrafish larvae, many biological processes occur, including inflammatory response, cell proliferation, neurogenesis, migration of surviving or newly generated cells, reformation of functional axons, and a global remodeling of neural processes circuits and spine tissues[6,7,9,10]. To be successfully orchestrated, these processes involve a finely regulated interaction between a range of cell types, extracellular matrix components, and biochemical signals[11,12]. Unraveling the details of this significant reorganization of a complex tissue such as the spinal cord requires the use and development of precise and controlled experimental approaches.

The primary experimental paradigm used to study spinal cord regeneration in zebrafish is to use surgical means to induce tissue damage by resection, stabbing, or cryoinjury[3,13]. These approaches have the disadvantage of requiring specific training in microsurgery skills, which is time-consuming for any new operator and may prevent their use in short-term projects. Furthermore, they usually induce damage to the surrounding tissues, which may influence regeneration.

Another approach is to induce cell damage chemically[14] or by genetic manipulations[15]. The latter allows for highly targeted damage. However, such a technique requires long preparatory work to generate new transgenic fish before doing any experiment, renewed each time a unique cell type is targeted.

There is, thus, the need for a method allowing targeted but versatile lesions suitable to a variety of studies in regeneration. A solution is to use a laser to induce localized damage in the tissue of interest[16,17,18,19,20]. Indeed, the use of laser-induced tissue damage presents a robust approach for generating spinal cord lesions with many advantages. The microscopes equipped with such laser manipulation modules allow specifying a customized shaped area where cell ablation will occur, with the extra benefit of temporal control. The size and position of the lesion can be thus adapted to address any questions.

The missing feature of most laser lesion systems is the possibility to induce injuries in a highly reproducible way for a series of larvae. Here an original protocol is described using a UV laser to induce semi-automated precise and controlled lesions in zebrafish larvae based on a microfluidic platform designed for automated larvae handling[21]. Moreover, in the system presented here, larvae are inserted in a glass capillary, which permits free rotation of the animal around its rostrocaudal axis. The user can choose which side of the larva to present to the laser while allowing fluorescence imaging to precisely target the laser beam and assess the damage after the lesion.

The protocol described here is used with a semi-automated zebrafish larvae imaging system combined with a spinning disk equipped with a UV laser (designated hereafter as the VAST system). However, the main points of the protocol and most of the claims of the technique are valid for any system equipped with a laser capable of cell ablation, including two-photon laser scanning microscopes, spinning-disk microscopes provided with a UV laser (FRAP module), or video-microscopes with a laser module for photo manipulation. One of the main differences between the VAST system and conventional sample handling will be that for the latter, mounting larvae in low-melting-point agarose on glass coverslips/glass-bottom Petri dishes in place of loading them in a 96-well plate will be required.

The benefits offered by this method open opportunities for innovative research on the cellular and molecular mechanisms during the regeneration process. Moreover, the high data quality allows for quantitative investigations in a multidisciplinary context.

PROTOCOL:

All animal studies were carried out with approval from the UK Home Office and according to its regulations, under project license PP8160052. The project was approved by the University of Edinburgh Institutional Animal Care and Use Committee. For experimental analyses, zebrafish larvae up to 5-day-old of either sex were used of the following available transgenic lines: Tg(Xla.Tubb:DsRed;mpeg1:GFP), Tg(Xla.Tubb:DsRed), Tg(betaactin:utrophin-mCherry), Tg(Xla.Tubb:GCaMP6s), and Tg(mnx1:gfp) (see **Supplementary File 1** regarding the generation of the transgenic zebrafish lines). A schematic of the protocol using the automated zebrafish larvae handling platform is shown in **Figure 1**. All custom software, scripts, and detailed experimental protocols used in this work are available at https://github.com/jasonjearly/micropointpy/.

1. Sample preparation

1.1. At 5 h post-fertilization, sort the embryos for the correct developmental stage[21]. Discard dead eggs and poorly developed and overdeveloped embryos.

1.2. At 3 days post-fertilization (dpf), anesthetize larvae by adding 2 mL of 0.4% aminobenzoic-acid-ethyl methyl-ester to 50 mL of fish facility water in a 90 mm Petri dish. Use animals raised with phenylthiourea (PTU) (see **Table of Material**) to prevent skin pigmentation if it is an issue, which is not the case for spinal cord injuries on 3 dpf larvae described in this protocol.

NOTE: This relatively high anesthetic concentration is used to prevent movements of the larvae following the laser impact.

1.3. Screen the embryos for fluorescent reporter expression (**Supplementary File 1**).

NOTE: A fluorescent reporter for the spinal cord (or other structure of interest) is often required to assess the efficiency of the injury. The use of tg(Xla.Tubb:DsRed) helps to identify the spinal cord.

1.4. Transfer the selected larvae into a 96-well plate for use in the VAST system (see **Table of Materials**) with 300 µL of fish facility water per well. Use the medium containing the anesthetic from the 90 mm Petri dish directly. Ensure to have only one larva per well. Prepare one extra empty 96-well plate to collect the lesioned larvae.

NOTE: If using another laser lesion system, mount the larvae in 1% Low-Melting Point (LMP) agarose gel in an appropriate observation chamber.

2. Microscope preparation

2.1. Switch on all the system components (VAST, microscope, laser, PC), including the laser for ablation.

2.2. Once the hardware is fully initialized, launch the microscope software, ImageJ/Fiji, a python integrated development environment (IDE), and the automated zebrafish imaging (VAST system) software if using this platform (see **Table of Materials**).

2.3. Set up the VAST software following the steps below.

2.3.1. When the VAST software launches, choose **Plate** on the first window and click on the **Done** button (**Figure 2A**). Another small window will pop up asking whether the capillary is empty and clean. Verify by looking at the image of the capillary if there are any air bubbles inside. If not, click on **Yes**. If there are any bubbles, click on **No** and follow step 2.3.2–2.3.3 (**Figure 2B**).

2.3.2. On the Large Particle (LP) Sampler window, click on **Prime** to remove air bubbles (**Figure 2C**).

2.3.3. Go to the main software window (with the capillary image) and right-click on the image. Select **Record empty capillary image** on the pop-up menu (**Figure 2B**).

2.3.4. In the **LP Sampler** window, go to the **File** menu and select the **Open Script** option. Choose a file containing the script corresponding to the experiment to be performed.

2.3.5. In the main VAST software window, go to **File** and choose **Open Experiment**. Choose the experiment file corresponding to the planned experiment.

NOTE: Ensure that the boxes Auto unload and Bulk output to waste are NOT checked.

2.4. Set up the microscope software for imaging.

2.4.1. Launch the microscope imaging software (see **Table of Materials**) to initialize the hardware. This may take a few minutes, depending on the system.

2.4.2. Go to the acquisition settings and set up the microscope for imaging the fluorophore expressed in the larvae. Use a 10x NA 0.5 water-dipping objective to ensure the focal volume is elongated enough along the optical axis to lesion the whole depth of the spinal cord or the targeted tissue.

2.5. Set up ImageJ/Fiji for laser lesions.

2.5.1. Go to the **File** menu, choose **New/Script** to open the script window.

2.5.2. In the **New** window, go to the **File** menu and choose **Open** to load the laser lesion script (Manual_MP_Operation.ijm).

2.6. Set up the Python IDE.

2.6.1. Launch the Python IDE.

2.6.2. Go to the **File** menu and choose **Open File** to load the script to manage the laser (Watch_for_ROIs_py3.py).

2.6.3. Go to the **Run** menu and choose **Run Without Debugging** to run the script. Check to ensure that a sequence of messages in the TERMINAL panel appears along with some noise while the laser attenuator initializes (**Figure 2D**).

3. Performing laser lesions on the VAST system

3.1. Center the capillary relative to the microscope objective by moving the stage by clicking on the arrow buttons on the main window of the VAST software (**Figure 2B**).

3.2. Focus on the top of the capillary by looking through the eyepieces and using the transmitted light of the microscope.

CAUTION: The capillary is very fragile and may break if touched by the objective. Move the microscope knob slowly when focusing in and out.

3.3. Place the 96-well plates on the plate holder of the LP Sampler of the VAST system. Place the plate containing larvae on the left holder and the plate for collection on the right. Ensure that

the plates are correctly oriented: the A1 well must be in the front-left corner of the holder.

3.4. In the VAST software, on the LP Sampler window, click on the **Plate Template** button and select all the wells containing larvae. Click on the **OK** button to validate and close the window (**Figure 2C**).

3.5. In LP Sampler window, click on the **Run Plate** button to start loading a larva.

NOTE: After some time, the larva should be visible in the capillary at position (predefined in the experiment definition file), allowing to injure the spinal cord. The VAST tray light will turn off after a few rotations to set the larva with the lateral side facing the microscope objective.

3.6. Go to the microscope software and click on the **Live** button to image the larva.

3.7. Turn the microscope focus knob until the spinal cord central canal is visible.

NOTE: It can be easier to focus using transmitted light first, and then refine with fluorescence.

3.8. Take a snapshot in fluorescence and save the image to a dedicated folder.

3.9. Open the image in ImageJ and adjust the contrast if required (using the **Image/Adjust/Brightness/contrast…** menu in ImageJ).

3.10. Click on the **Region of Interest (ROI)** line tool and draw a short line (20 µm) centered on the spinal cord (**Figure 3A**).

3.11. Switch the microscope to the 100% reflective mirror position.

3.12. Load the ImageJ script and click on the **Run** button. Use the following parameters: Repetition - 2; Sample - 1; Width - 40-micron; Attenuation - 89 (Full laser power) (**Figure 3C**).

3.13. When the laser shot sequence is finished, switch to fluorescence imaging on the imaging software and adjust the focus if required.

NOTE: A shift in focus is often observed due to tail displacement during laser exposure.

3.14. Take a new snapshot and save it.

3.15. Open this new image in ImageJ and draw a new line that should be larger than the spinal cord itself (~80 µm), starting below the ventral side of the spinal cord in the upper part of the notochord and going towards the dorsal side to end in the space between the spinal cord and the skin (**Figure 3B**).

3.16. Switch the microscope to the 100% reflective mirror position.

3.17. Go to the ImageJ script window and click on the **Run** button. Use the following parameters: Repetition - 2; Sample - 1; Width - 40 microns; Attenuation - 89 (Full laser power).

3.18. After the (longer) laser shot sequence is finished, verify the transection quality by imaging fluorescence and focusing. Ensure that no cell or axons remain intact in the lesion site, which should appear as a dark or as a faint and homogeneous fluorescent area (**Figure 3D**, bottom panel).

3.19. Collect the lesioned larvae into the empty 96-well plate (with the same well co-ordinates as that of the original well) by going to the main VAST software window and clicking on the **Collect** button.

3.20. Switch back on the VAST system light by clicking on the check box **Tray Light** on the bottom left of the window.

3.21. Repeat step 3.3–3.17 for each new larva to be injured.

4. Post-lesion handling and additional experiments

4.1. Take out larvae from the 96-well plate as soon as possible and transfer them to a clean Petri dish with fresh fish facility water for the larvae to recover post-lesion. Put the Petri dish in an incubator at 28 °C.

NOTE: The damage often continues to propagate in the first hour after the lesion. The actual extent of the lesion should thus be assessed by fluorescence imaging after a delay of approximately 1 h.

5. Troubleshooting

5.1. If air bubbles are present in the tubes and capillary of the VAST system, click on the **Prime** button on the LP Sampler window to remove them.

5.2. Consider the unsuccessful lesions (as assessed from the remaining fluorescence in the lesion site, apart from the expected residual and homogenous background), which can be due to several reasons mentioned below.

5.2.1. Low laser power: When this happens, try with a higher value.

NOTE: The VAST system is equipped with a dye laser. This implies that the concentration of the dye solution used for laser light generation can change with time, leading to a decrease in laser power. Replacing with a fresh solution usually solves the problem[22].

5.2.2. Poor calibration: When this happens, verify the calibration and power of the laser system as per step 5.2.2.1–5.2.2.4. If not calibrated correctly, the laser won't be directed to the desired location, thus leading to unsuccessful lesions or undesired damage in adjacent tissues.

5.2.2.1. Place a mirror slide on top of the capillary chamber. Focus on the coated side (it should face the objective). Use a previous default in the slide to focus more easily.

5.2.2.2. Apply a pattern of laser ablation using a calibration script.

5.2.2.3. Assess the quality of the pattern. The spots or lines should appear sharp and not blurry.

5.2.2.4. Use a ramp with increasing power to evaluate whether the laser power has changed compared to the previous sessions.

5.2.3. Larval movement during lesions: Larvae respond differently to anesthesia; thus, the laser lesion may trigger movements of the tail during the process, thus preventing a successful transection. When this happens, take an extra iteration of the laser lesion steps to complete it while still avoiding damage to the surrounding tissues.

5.2.4. Bad focus: When this occurs, focus on the middle of the central canal to get the best results.

5.2.5. ROI drawing, position, and size: The position and size of the ROI are critical for successful transections. The ROI should be larger than the spinal cord and centered on the center of the spinal cord. To solve this, start to draw the ROI from the ventral side of the spinal cord and go up toward the dorsal side to obtain successful transection. This is likely due to tail movements triggered by the sequence of laser shots during the ablation procedure.

REPRESENTATIVE RESULTS:

Validation of spinal cord transection

Structural and functional investigations were performed to assess whether the protocol allows a complete spinal cord transection.

First, to verify that the loss in fluorescence at the lesion site was due to neuronal tissue damage and not fluorescence photobleaching from the laser illumination, immunostaining using an antibody against acetylated tubulin (see **Table of Materials** and **Supplementary File 1**) was performed. A complete disruption of the axons between the caudal and rostral sides of the lesion was observed, confirming the complete transection of the spinal cord (**Figure 4B**). A successful spinal cord transection should not leave any remaining neuronal projection across the lesion site (see **Figure 4C** for an example of an unsuccessful lesion). Using this technique, the success rate of spinal cord laser lesions was estimated to be 75% (four incomplete transections in 16 animals).

The loss of functionality after laser lesion was investigated using calcium imaging. On intact fish, the spontaneous co-ordinated neuronal network activity generates fluorescence peaks along the whole spinal cord. A successful transection would interrupt the propagation of this activity between both sides of the lesion. To control the quality of the spinal cord transection, laser lesions were performed on tg(Xla.Tubb:GCaMP6s) larvae at 3 dpf. After collection in a new multi-well plate, larvae were mildly anesthetized. They were mounted on a glass coverslip in low-melting-point agarose to perform fluorescence time-lapse recordings on a confocal microscope from 3 h post-injury. A loss of activity on the caudal side of the lesion site was observed. Indeed, the quantification of fluorescence shows that spikes due to the fish's spontaneous activity were only present on the rostral side after injury but occurred in a co-ordinated manner in the equivalent rostral and caudal positions in intact fish (**Figure 4D,E**). The low residual signal on the caudal side after injury was likely due to the activity of sensory neurons (probably Rohon-Beard sensory neurons on the caudal side of the spinal cord[23]) in reaction to the tail movement induced by muscle contraction on the rostral side.

Regeneration processes induced by laser lesions

After 24 hours post-injury (hpi), the wound started to close, leading to a partial restoration of the initial structure of the spinal cord after 48 h (**Figure 5D**). Using calcium imaging, a partial functional reconnection was confirmed (**Figure 5E,F**) after 48 hpi. The calculation of the ratio (named Connectivity Restoration Index by the authors) between the amplitude of the spikes in the caudal area and the rostral area (**Figure 5G**), showed an increase between 3, 24, and 48 hpi, as expected during spinal cord regeneration.

Laser lesions trigger an immune response

Macrophage (mpeg1:GFP + cells) recruitment was observed after laser lesions using tg(Xla.Tubb:DsRed;mpeg1:GFP) larvae laser lesions (**Figure 5H,I**). This is consistent with previous studies by the authors using manual lesions demonstrating the essential role of macrophages for successful regeneration of the spinal cord in zebrafish larvae[6,24]. This observation indicates that immune reactions can be studied after laser injury and corroborates that tissue damage occurred.

Laser lesions and manual lesions trigger increased neurogenesis in the spinal cord

Previous studies have used manual lesions to study the neurogenesis that occurs following a spinal cord injury[6,15]. Laser lesions could be a valuable tool to study this phenomenon. A previously published experiment showed increased neurogenesis following a manual spinal cord injury compared to unlesioned controls[15]. Here tg(mnx1:gfp) fish were used as motor neurons and were fluorescently labeled. Anti-GFP antibody staining was used to improve the visibility of GFP in the larvae. This was combined with EdU staining[25] (see **Supplementary File 1**), which labels newly generated neurons. EdU was added immediately following an injury at 3 dpf, meaning that any cells labeled with EdU were generated post-injury. Therefore, cells that display colocalized staining represent new motor neurons that are born after spinal cord injury. The number of colocalized cells on either side of the injury site, or in an area corresponding to the location and size of the injury site in unlesioned controls (captured in two 50 µm windows) were counted, and the difference in the mean numbers of colocalized cells was analyzed using a one-way ANOVA[26].

This protocol was used on manually and laser lesioned larvae to compare the effects of each lesion method on neurogenesis (**Figure 6**). No difference was observed in the number of labeled cells between manual and laser lesions. Unlesioned fish displayed fewer double-labeled cells than lesioned fish in both lesion conditions (**Figure 6D**). This is consistent with previous findings showing increased neurogenesis in manually lesioned fish compared to unlesioned fish[15].

These results support the calcium imaging and acetylated tubulin staining results, as the laser injury elicits a regeneration response comparable to a manual lesion. This indicates that the laser lesion is not simply bleaching the fluorescence in the cells but results in an injury that triggers the same cellular responses that a manual lesion does.

Laser lesions result in less skin and muscle damage than manual lesions

Manual lesions often result in large amounts of muscle and skin damage. In contrast, laser lesions can be targeted more specifically to the spinal cord, reducing the damage to other tissues. To illustrate this, Tg(beta-actin:utrophin-mCh) larvae were used to perform manual and laser lesions. This line fluorescently labels an F-actin-binding protein, allowing the visualization of spinal cord cells and muscle fibers. The larvae were then live mounted and imaged (**Figure 7A,B**). **Figure 7A** shows the damage to the spinal cord. The lack of utrophin in the injury site in both laser and manual lesion conditions suggests that both lesion methods have damaged the cells in the spinal cord. **Figure 7B** shows the muscle damage. There is a clear chevron-like structure to the myotomes in the unlesioned condition, and bundles of actin fibers are visible. There is a visible disruption to the myotome shape in the manual lesion condition, and fewer actin fibers are present. This demonstrates significant muscle damage. However, in the laser lesion condition, the chevron structure of the myotome is maintained. There is some damage to muscle fibers, but this is contained within one or two myotomes compared to within four in the manual lesion condition. In addition, there is minor skin damage in the laser lesion condition compared to the manual lesion condition, as shown in images taken on a stereo microscope in **Figure 7C**.

Altogether, these results demonstrate that reproducible, semi-automated laser lesions have the potential to be a powerful tool to study neural regeneration in zebrafish.

FIGURE LEGENDS:

Figure 1: Schematic of the semi-automatic laser-injury workflow. Three days post-fertilization (dpf), larvae are loaded into a 96-well plate and placed on the automated larvae handling platform. Then, each larva is loaded into a capillary placed under a 10x NA 0.5 lens on an upright microscope for imaging and laser lesion. After lesions, larvae are unloaded to a new 96-well plate for collection and further experiments. On the top, transmitted and fluorescence images of tg(Xla.Tubb:DsRed) 3 dpf larvae before and after laser lesion (scale bar = 50 μm). Larvae are oriented rostral left and dorsal up (for all figures).

Figure 2: Software start-up for the semi-automated zebrafish larvae imaging system and laser control system. (**A**) VAST software at start-up. (**B**) The main window of the VAST software shows

the empty capillary. (**C**) LP Sampler window with a blank plate template. (**D**) The view of python IDE with the Watch_for_ROIs_py3.py script running. The orange rectangle points out the terminal tab with messages displayed during the initialization of the laser attenuator.

Figure 3: Example of laser lesion sequence on tg(Xla.Tubb:DsRed) 3 dpf larvae. (**A**) The first step of laser lesion using a 20 µm line after selecting the line ROI tool from the ImageJ toolbar. (**B**) Second step with an 80 µm line for complete transection of the spinal cord. (**C**) View of the script used for controlling the laser from ImageJ. (**D**) The sequence of images during laser lesions. Top: before lesion; Middle: immediately after the first step; Bottom: immediately after the second step (scale bar = 50 µm).

Figure 4: Acetylated tubulin immunostaining (A–C) and calcium imaging (D,E) indicate that laser lesion entirely disrupts the continuity of spinal tissue. (**A**) Intact spinal cord. (**B**) Complete transection of the spinal showing a complete disruption of the spinal cord tissue along both the dorsal-ventral and medial-lateral axes. (**C**) Incomplete transection. (scale bar = 50 µm). (**D**) Transected spinal cord on a tg(Xla.Tubb:GCaMP6s) 3 dpf larva. The rectangles show the ROIs used to quantify the fluorescence intensity in the lesion's rostral (blue) and caudal (orange) sides. (**E**) Graph of the fluorescence intensity changes over time in the rostral and caudal analysis ROIs.

Figure 5: Laser injury elicits an immune response and leads to successful anatomical and functional recovery. (**A–D**) The maximum intensity projection fluorescence images of a tg(Xla.Tubb:DsRed) 3dpf larva before (**A**) and at different times after the laser lesion: after 3 h (**B**), after 24 h (**C**), and after 48 h (**D**). (**E–G**) The use of calcium imaging to assess the function restoration. (**E**) Lesioned tg(Xla.Tubb:GCaMP6s) larva with analysis ROIs. (**F**) Graph of the fluorescence intensity changes over time in the rostral and caudal analysis ROIs. (**G**) Quantification of the ratio between caudal and rostral spike amplitudes (Connectivity Restoration Index) at 3, 24, 48 h post-lesion (N = 3). (**H–I**) Characterization of the immune response after lesion. (**H**) Fluorescence images of unlesioned (left) and lesioned (right) tg(Xla.Tubb:DsRed;mpeg1:GFP) 3 dfp larva showing the accumulation of macrophages (mpeg1+ cell, green) at 6 hpi. (**I**) Quantification of the number of macrophages at 6 h post-lesion in injured and intact larvae (N = 3) (scale bars = 50 µm).

Figure 6: Lesion-induced generation of motor neurons is comparable between laser and manual lesion. (**A–C**) Images from the ApoTome microscope of tg(mnx1:gfp) 5 dpf larvae with EdU staining, in laser lesion (**A**), manual lesion (**B**), and unlesioned (**C**) conditions. Arrowheads denote cells double-labeled for both markers. Scale bar = 100 µm. (**A'–C'**) Higher magnification of double-labeled cells denoted by white boxes. (**D**) Quantification of cell counts for the number of colocalized cells in each larva. 50 µm windows were placed on either side of the injury site, and colocalized cells were counted in all Z-stack images. One-way ANOVA was performed with Tukey's posthoc test[27]. No significant difference between laser and manual lesions ($p = 0.909$). Significantly fewer mnx1:gfp+/EdU+ cells in unlesioned controls compared to laser lesion (2.4 fold change, $p = 0.011$) and manual lesion (2.3 fold change, $p = 0.018$).

Figure 7: Laser lesion induces less muscle and skin damage than the manual lesion. (**A–B**) Single Z-stack images of tg(beta-actin:utrophin-mCherry) 3 dpf larvae in the unlesioned, manual lesion and laser lesion conditions, taken on the confocal microscope at 20x magnification. White arrows denote the injury site. Scale bar = 50 µm. (**A**) denotes Z-stacks where the spinal cord and notochord are visible. SC labels the spinal cord, and NC labels the notochord. (**B**) denotes Z-stacks where the muscle fibers are visible. (**C**) Images were taken on the stereo microscope of 3 dpf larvae in the unlesioned, manual lesion, and laser lesion conditions. Larvae were pinned to a platform using tungsten wire pins (visible in laser lesion image). The black box denotes the lesion site. Scale bar = 50 µm.

Supplementary File 1: The experimental details of the protocol. The generation of the transgenic zebrafish lines, manual spinal cord injuries, acetylated-tubulin immunohistochemistry, Hb9/EdU staining, imaging, and image processing and analysis are described.

DISCUSSION:

There is an urgent need for a deeper understanding of the processes at play during regeneration in zebrafish. This animal model offers many benefits for biomedical research, in particular for spinal cord injuries[1]. Most of the studies involve manual lesions that require a well-trained operator and induce multi-tissue damage. A laser lesion protocol is presented here, allowing control over the lesion characteristics and reduced damage to the surrounding tissues. Furthermore, this technique is easy enough to be successfully used by relatively untrained experimenters.

Critical steps in the protocol are the calibration of the laser and the definition of ROIs. In practice, the calibration is very stable (even for months), and once the right size and position of the ROI have been determined, the use of this technique is straightforward. Although the protocol described how to perform the lesions on specific equipment, most of the benefits of laser lesions are available for different systems, such as a spinning-disk microscope.

The main limitations of this protocol are the need to use a fluorescence reporter of the spinal cord and the time required to perform the lesions (~5 min/fish). The latter is compensated for by high reproducibility requiring fewer animals. However, manual lesions are still viable for applications such as drug testing, where many lesioned animals are needed. As shown here, the extent of lesion-induced neurogenesis is comparable between laser and manual lesions.

However, laser injury has enormous potential applications, some of them related to the unique benefits offered. For example, a rotating capillary allows performing lesions in a large variety of positions in a controlled way. For example, it could be used to induce single neuron axotomy in Mauthner cells (data not shown), as has also been demonstrated in the work of Bhatt et al.[15]. This would not be possible using manual lesions.

The results also demonstrate that the damage is mainly contained to the spinal cord, with minimal damage to surrounding tissues. This could mean that cellular responses seen following a laser lesion are more likely to be attributed to the spinal cord specifically rather than signaling

from other damaged tissues. It also could mean that laser lesioned larvae are more able to withstand further preparations for experiments. For example, dissection for electrophysiology involves removing the trunk skin using forceps[28,29,30], which would result in high mechanical pressure placed on the already delicate injury site and risk any axonal connections to be broken again. The integrity of skin and muscle tissue seen in laser-lesioned larvae could protect the lesion site from further damage and result in a more accurate representation of the level of regeneration achieved.

Moreover, the improved localization of damage after laser injury limits the extension of coupling between different regeneration processes, which may mask more subtle processes when using manual lesions. The approach to experimental injury in the larval zebrafish described here may open a range of new investigations in the context of quantitative biology, biological physics, and computational biology.

ACKNOWLEDGMENTS:

This study was supported by the BBSRC (BB/S0001778/1). CR is funded by the Princess Royal TENOVUS Scotland Medical Research Scholarship Programme. We thank David Greenald (CRH, University of Edinburgh) and Katy Reid (CDBS, University of Edinburgh) for the kind gift of transgenic fish (See **Supplementary File**). We thank Daniel Soong (CRH, University of Edinburgh) for the kind access to the 3i spinning-disk confocal.

DISCLOSURES:

The authors have nothing to disclose.

REFERENCES:

1. Becker, C. G., Becker, T. Adult zebrafish as a model for successful central nervous system regeneration. *Restorative Neurology and Neuroscience*. **26** (2–3), 71–80 (2008).
2. Ohnmacht, J. et al. Spinal motor neurons are regenerated after mechanical lesion and genetic ablation in larval zebrafish. *Development*. **143** (9),1464–1474 (2016).
3. Anguita-Salinas, C. et al. Cellular dynamics during spinal cord regeneration in larval zebrafish. *Developmental Neuroscience*. 41 (1–2), 112–122 (2019).
4. Chapela, D. et al. A zebrafish drug screening platform boosts the discovery of novel therapeutics for spinal cord injury in mammals. *Scientific Reports*. **9**, 1–12 (2019).
5. Schlüßler, R. et al. Mechanical mapping of spinal cord growth and repair in living zebrafish larvae by brillouin imaging. *Biophysical Journal*. **115** (5), 911–923 (2018).
6. Cavone, L. et al. A unique macrophage subpopulation signals directly to progenitor cells to promote regenerative neurogenesis in the zebrafish spinal cord. *Developmental Cell*. **56** (11), 1617–1630 (2021).
7. Keatinge, M. et al. CRISPR gRNA phenotypic screening in zebrafish reveals pro-regenerative genes in spinal cord injury. *PLoS Genetics*. **17** (4), 1–21 (2021).
8. https://nc3rs.org.uk/
9. Hui, S. P. et al. Genome wide expression profiling during spinal cord regeneration identifies comprehensive cellular responses in Zebrafish. *PLOS ONE*. **9** (1), 1–23 (2014).

10. Vasudevan, D. et al. Regenerated interneurons integrate into locomotor circuitry following spinal cord injury. *Experimental Neurology*. **342**, 1–10 (2021).
11. Becker, T., Becker, C. G. Dynamic cell interactions allow spinal cord regeneration in zebrafish. *Current Opinion in Physiology*. **14**, 64–69 (2020).
12. Wehner, D. et al. Wnt signaling controls pro-regenerative Collagen XII in functional spinal cord regeneration in zebrafish. *Nature Communications*. **8** (126), 1–16 (2017).
13. Briona, L. K., Dorsky, R. I. Spinal cord transection in the larval Zebrafish. *Journal of Visualised Experiments: JoVE*. **87** (2014).
14. Kamei, C. N., Liu, Y., Drummond, I. A. Kidney regeneration in adult Zebrafish by gentamicin induced injury. *Journal of Visualized Experiments: JoVE*. **102** (2015).
15. Bhatt, D. H., Otto, S. J., Depoister, B., Fetcho, J. R. Cyclic AMP-induced repair of zebrafish spinal circuits. *Science*. **305** (5681), 254–258 (2004).
16. Xu, Y., Chen, M., Hu, B., Huang, R., Hu, B. In vivo imaging of mitochondrial transport in single-axon regeneration of zebrafish mauthner cells. *Frontiers in Cellular Neuroscience*. **11** (4), 1–12 (2017).
17. Nichols, E. L., Smith, C. J. Functional regeneration of the sensory root via axonal invasion. *Cell Reports*. **30** (1), 9–17 (2020).
18. Ellström, I. D. et al. Spinal cord injury in zebrafish induced by near-infrared femtosecond laser pulses. *Journal of Neuroscience Methods*. **311**, 259–266 (2016).
19. Green, L. A., Nebiolo, J. C., Smith, C. J. Microglia exit the CNS in spinal root avulsion. *PLOS Biology*. **17** (2), 1–30 (2019).
20. Early, J. J. et al. An automated high-resolution in vivo screen in zebrafish to identify chemical regulators of myelination. *eLife*. 1–31 (2018).
21. Kimmel, C. B., Ballard, W. W., Kimmel, S. R., Ullmann, B., Schilling, T. F. Stages of embryonic development of the Zebrafish. *Developmental Dynamics*. **203**, 253–310 (1995).
22. https://andor.oxinst.com/downloads/view/andor-micropoint-manual
23. Knafo, S. et al. Mechanosensory neurons control the timing of spinal microcircuit selection during locomotion. *eLife*. **6**, e25260 (2017).
24. Tsarouchas, T. M. et al. Dynamic control of proinflammatory cytokines Il-1β and Tnf-α by macrophages in zebrafish spinal cord regeneration. *Nature Communications*. **9** (2018).
25. Salic, A., Mitchison, T. J. A chemical method for fast and sensitive detection of DNA synthesis in vivo. *Proceedings of the National Academy of Sciences of the United States of America*. **105** (7) 2415–2420 (2008).
26. Howell, D. Statistical methods for psychology. Duxbury. 324–325 (2002).
27. Tukey, J. Comparing individual means in the analysis of variance. *Biometrics*. **5** (2), 99–114 (1949).
28. Song, M., Mohamad, O., Chen, D., Yu, S. P. Coordinated development of voltage-gated Na+ and K+ currents regulates functional maturation of forebrain neurons derived from human induced pluripotent stem cells. *Stem Cells and Development*. **22** (10), 1551–1563 (2013).
29. Hong, S., Lee, P., Baraban, S., Lee, L. P. A novel long-term, multi-channel and non-invasive electrophysiology platform for Zebrafish. *Scientific Reports*. **6**, 1–10 (2016).
30. Menelaou, E., McLean, D. L. Hierarchical control of locomotion by distinct types of spinal V2a interneurons in zebrafish. *Nature Communications*. **10**, 1–12 (2019).

Figure 1

Click here to access/download;Figure;Figure1.pdf

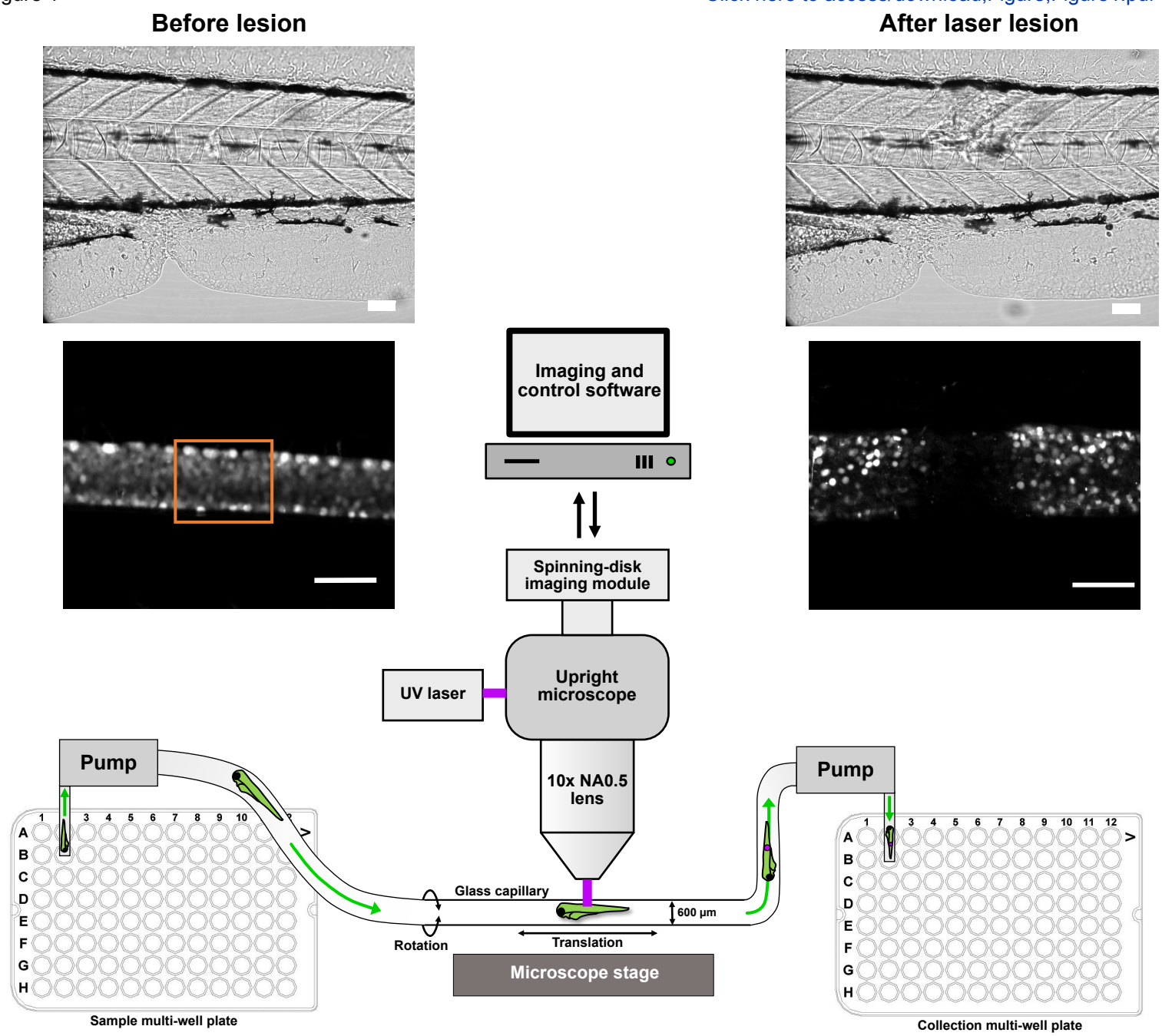

Figure 2

Click here to access/download;Figure;Figure2.pdf

A

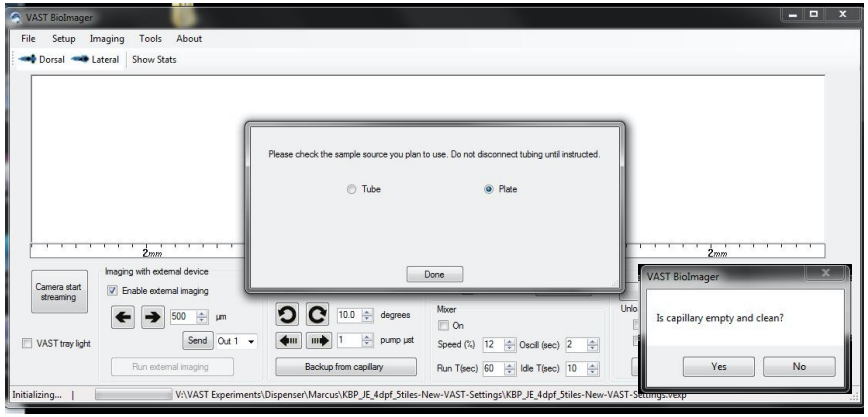

B

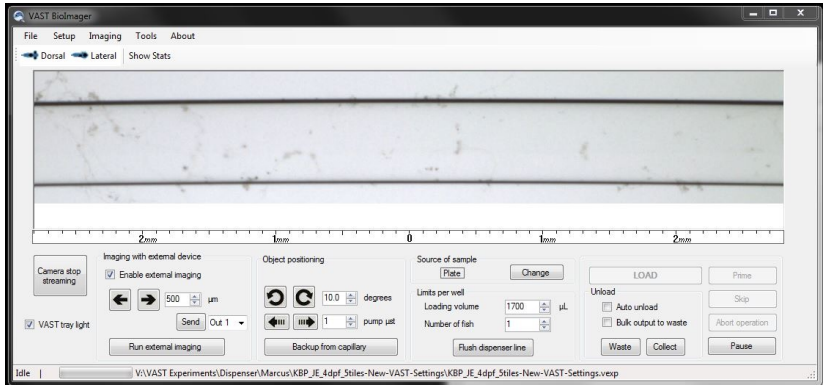

C

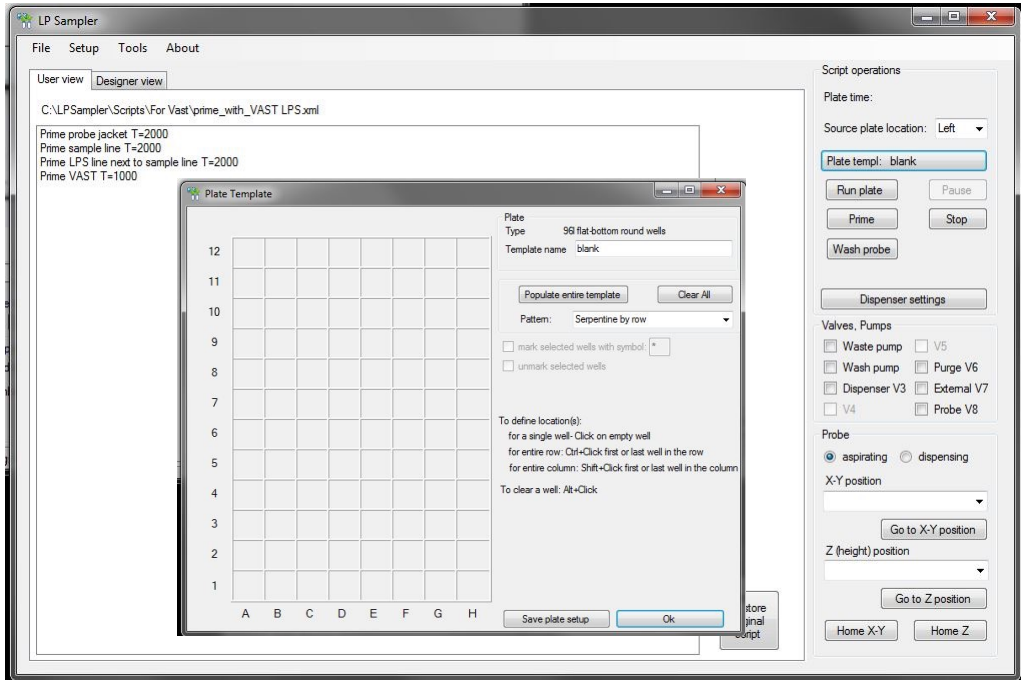

D

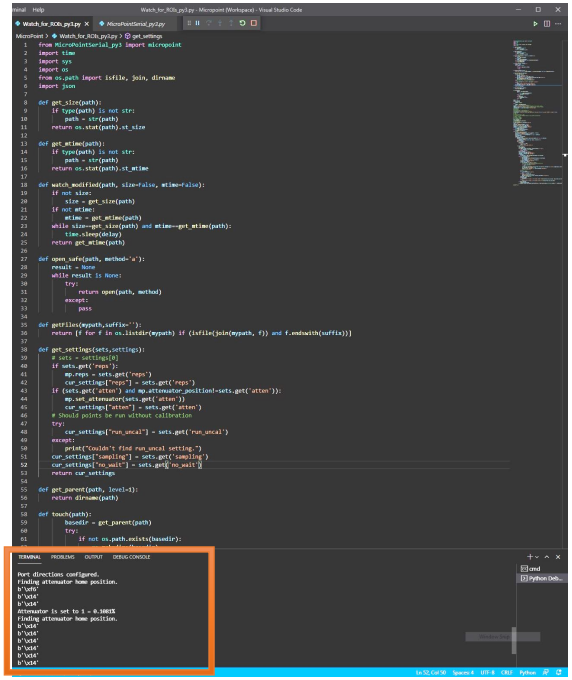

Figure 3

Click here to access/download;Figure;Figure3.pdf

A

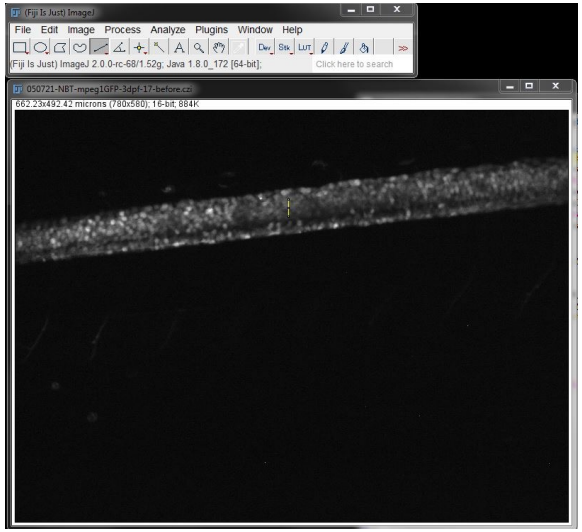

B

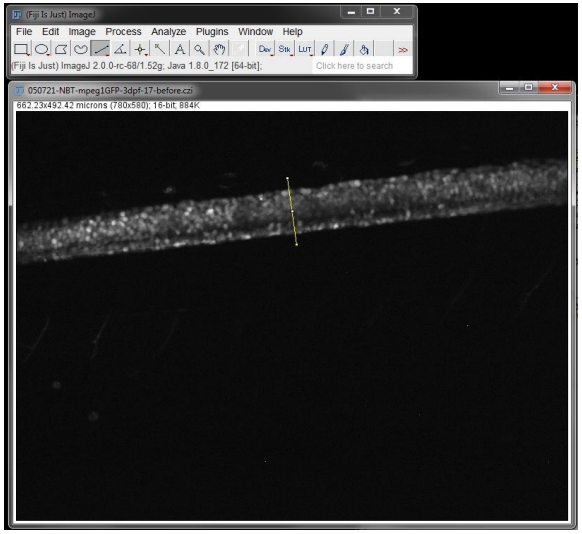

C

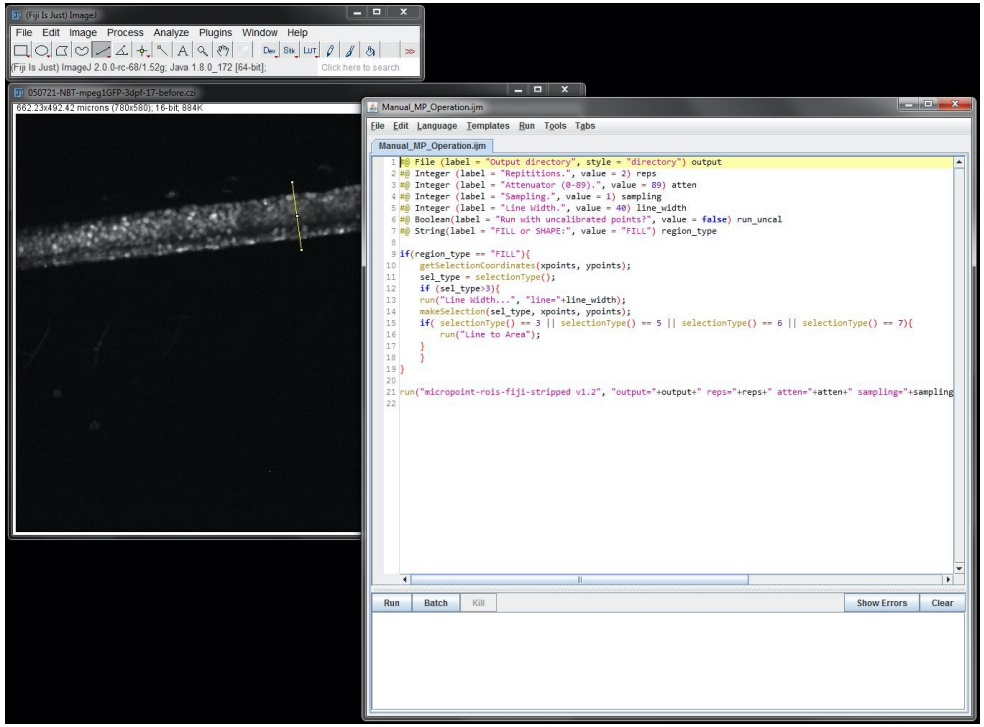

D

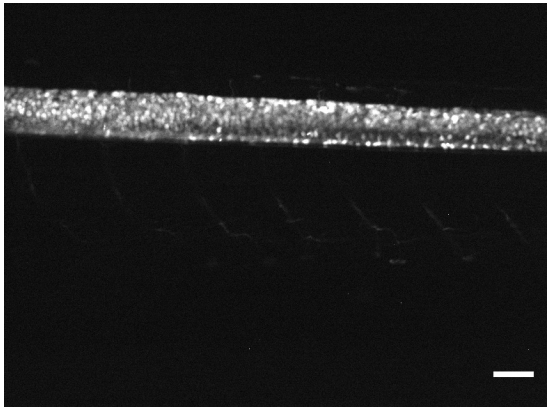

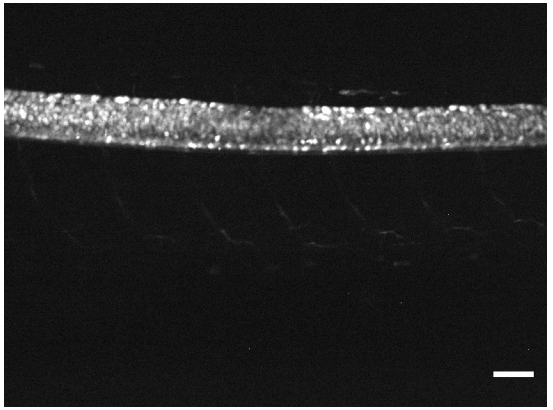

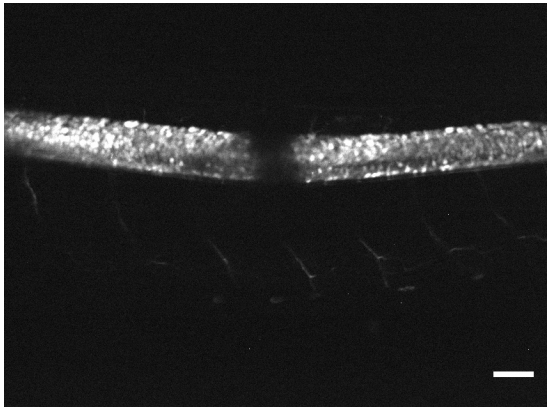

Figure 4

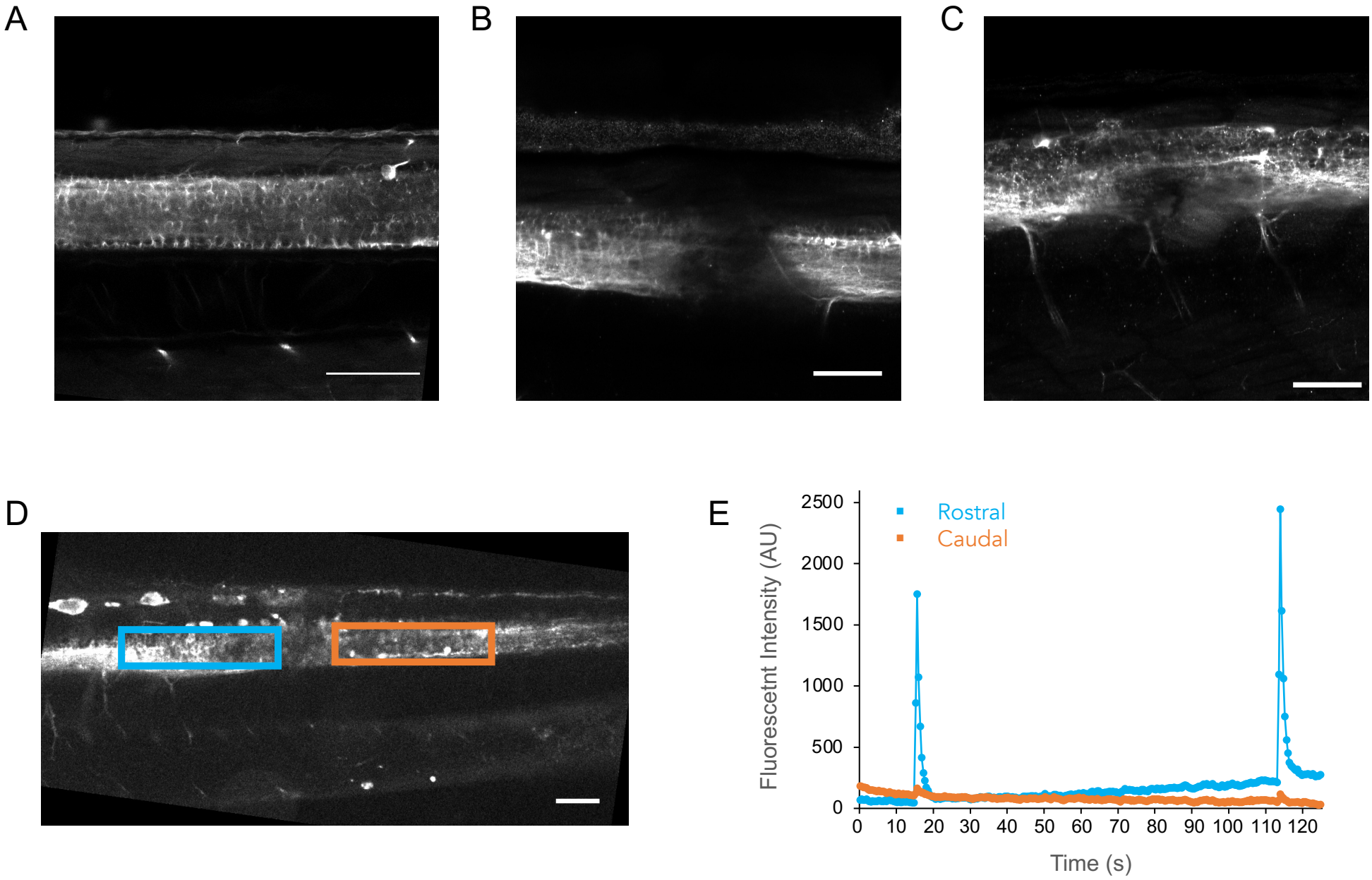

Figure 5

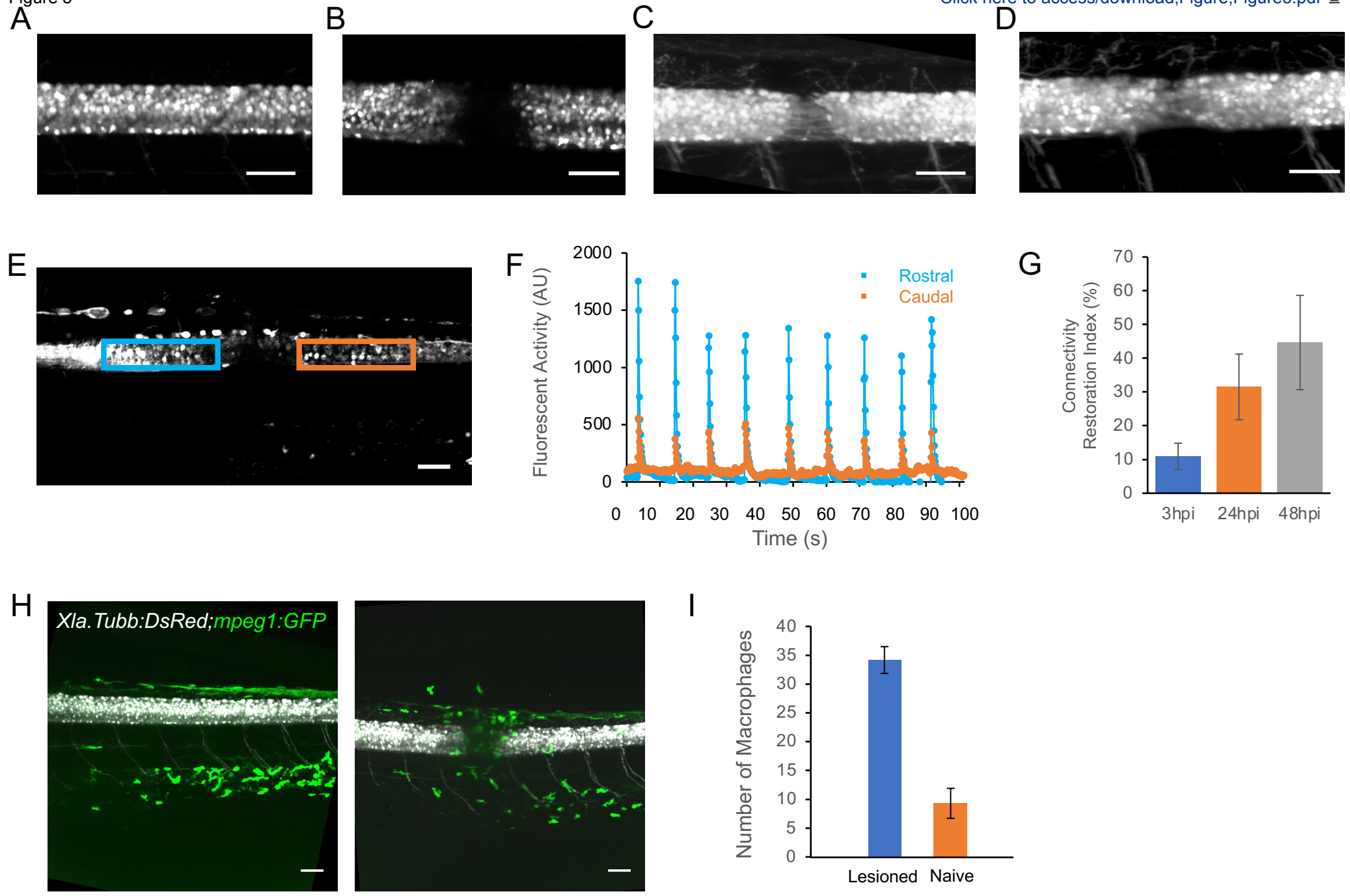

Figure 6

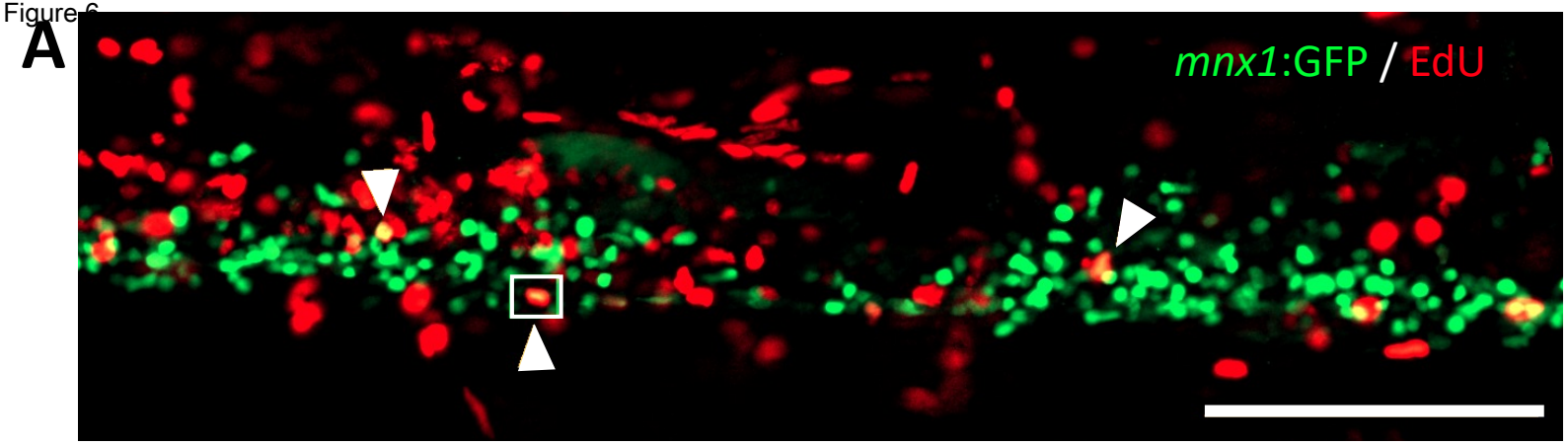

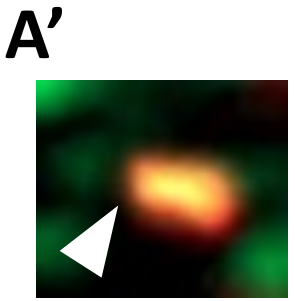

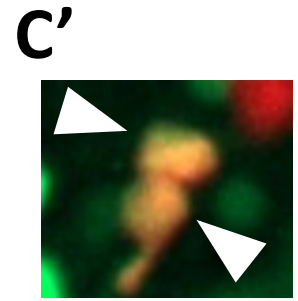

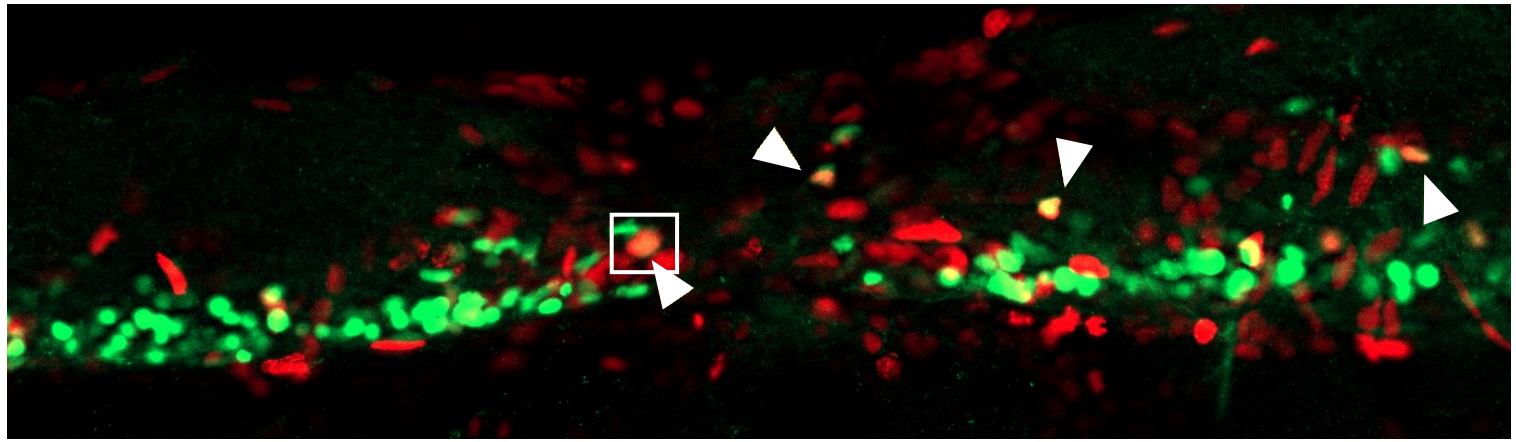

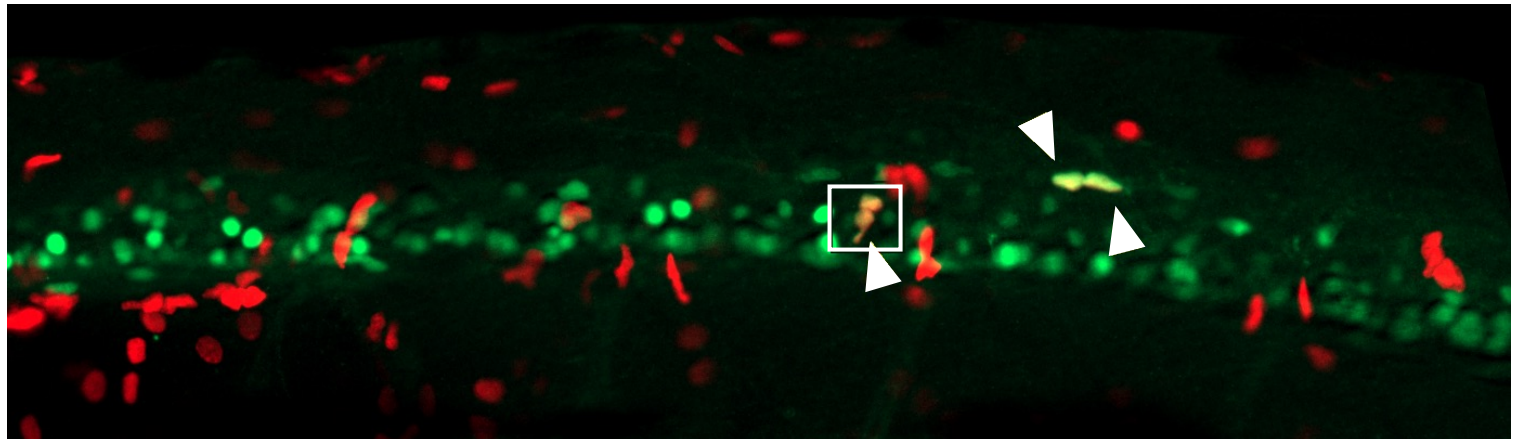

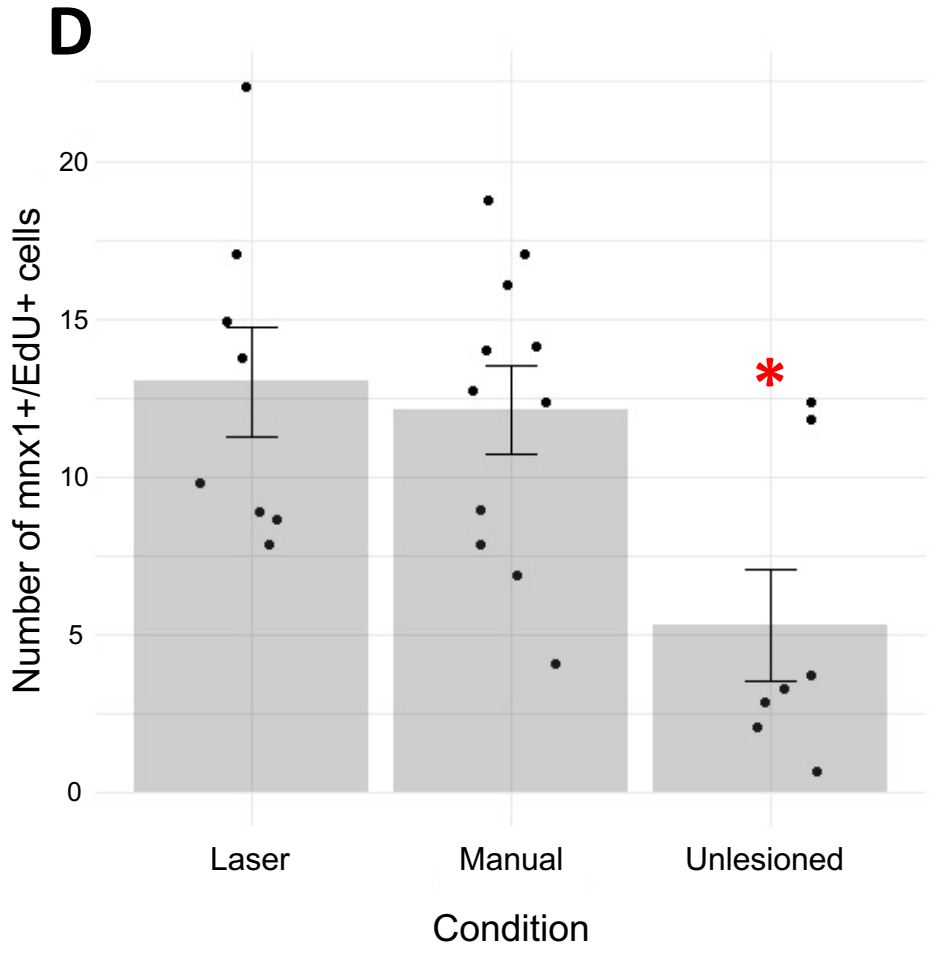

Figure 7

Click here to access/download;Figure;Figure7.pdf

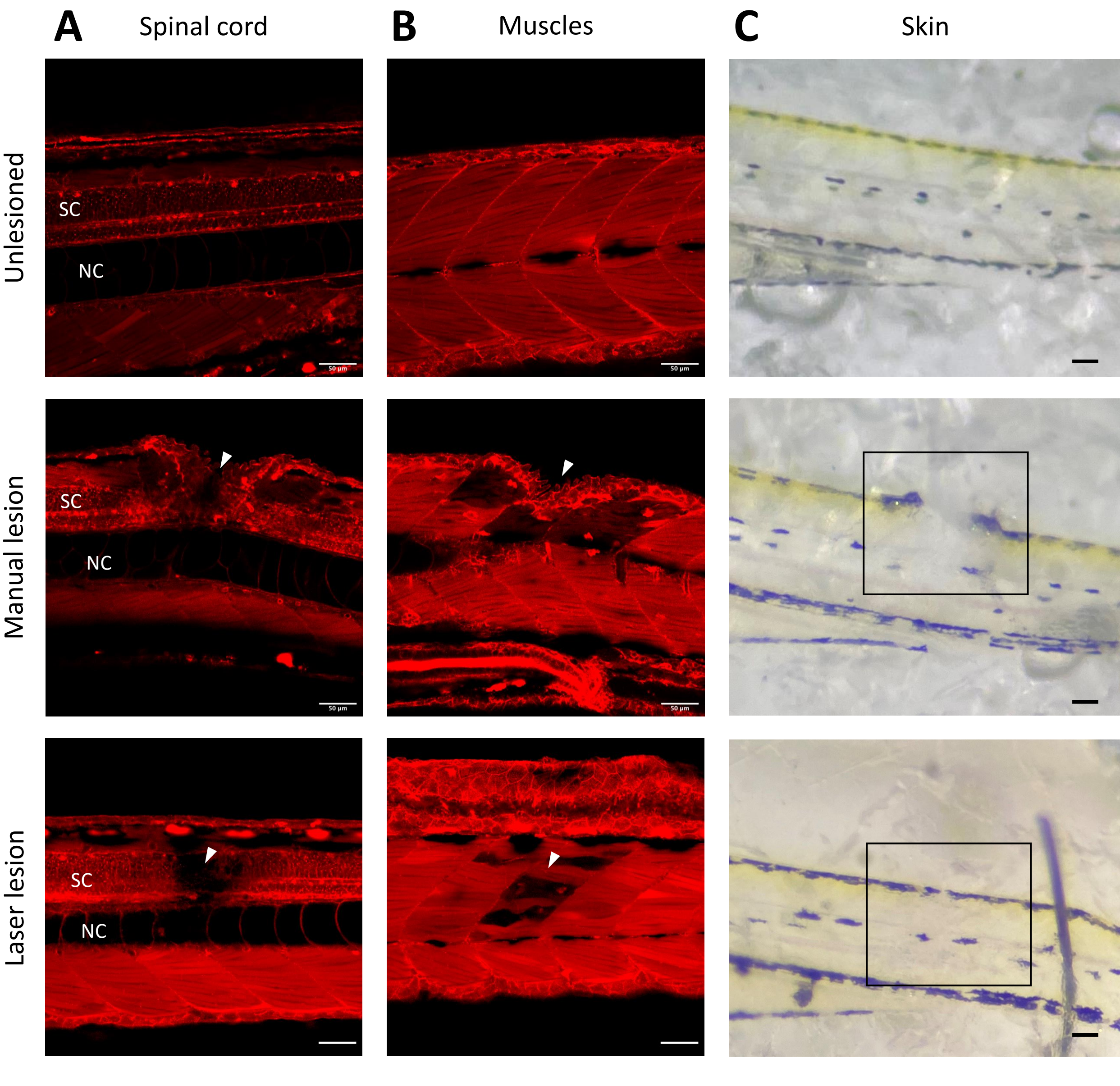

JOVE - 63259_R0 Rebuttal letter

Dear Dr. El-Daher,

Your manuscript, JoVE63259 "Controlled semi-automated lased-induced injuries for studying spinal cord regeneration in zebrafish larvae," has been editorially and peer reviewed, and the following comments need to be addressed. Note that editorial comments address both requirements for video production and formatting of the article for publication. Please track the changes within the manuscript to identify all of the edits.

After revising and uploading your submission, please also upload a separate rebuttal document that addresses each of the editorial and peer review comments individually.

Your revision is due by **Oct 18, 2021**.

To submit a revision, go to the JoVE submission site and log in as an author. You will find your submission under the heading "Submission Needing Revision". Please note that the corresponding author in Editorial Manager refers to the point of contact during the review and production of the video article.

Best,

Nilanjana Saha, PhD
Review Editor
JoVE

Dear Nilanjana,
We thank you for your encouragement to submit the present appeal. We also thank you and the two expert referees for your time and extensive effort to improve our manuscript. We are grateful to Reviewers 1 and 2 for their positive appreciation that “This is an important step forward” and “It is a very strong paper of wide use to the zebrafish community, and possibly other scientists who utilize transparent organisms.”

The scope of our paper is the demonstration of a protocol allowing reproducible tissue-specific injuries using laser ablation combined with a semi-automated zebrafish larvae handling platform. Additionally, we show benefits from the application of this method for studying regeneration in the spinal cord and the use of complementary approach to assess the success of transections. Lastly, we demonstrate that this protocol triggers an immune response, thus expanding the use of this technique to studying immune reactions in various experimental conditions, such as in drug screening assays.
After carefully reading the comments of the editor and the reviewers, we provide a revised manuscript addressing each comment, as you can see form our-point-by-point response below.

Looking forward to hearing from you.

Best regards,
Francois El-Daher

Editorial comments:

Changes to be made by the Author(s):

1. Please take this opportunity to thoroughly proofread the manuscript to ensure that there are no spelling or grammar issues.

> We proofread the manuscript and corrected those issues.

2. Please rephrase the Summary to clearly describe the protocol and its applications in complete sentences between 10-50 words: “The present protocol describes. …”. Here the word limit is exceeding.

> The word count has been reduced and the text rephrased.

3. Please revise the text to avoid the use of any personal pronouns (e.g., "we", "you", "our" etc.).

> All personal pronouns have been removed.

4. JoVE cannot publish manuscripts containing commercial language. This includes trademark symbols (™), registered symbols (®), and company names before an instrument or reagent. Please remove all commercial language from your manuscript and use generic terms instead. All commercial products should be sufficiently referenced in the Table of Materials. For example: ZEISS

> All mentions of commercial product have been removed.

5. Line 116-124: Please move this to the Introduction section. The Protocol should contain only action items written in the imperative tense that direct the reader to do something. Any text that cannot be written in the imperative tense may be added as a “Note.” However, notes should be concise and used sparingly.

> The section has been moved.

6. Please note that your protocol will be used to generate the script for the video and must contain everything that you would like shown in the video. Please ensure you answer the “how” question, i.e., how is the step performed? Alternatively, add references to published material specifying how to perform the protocol action. There should be enough detail in each step to supplement the actions seen in the video so that viewers can easily replicate the protocol.

> We ensured that every step was clearly detailed.

7. Please add more details to your protocol steps:
Step 1.1: How the 50% epiboly is ensured?
Step 2.2: Please provide the python scripts as Supplementary files or provide the Github repository link.

> Step 1.1: Reference to epiboly has been removed as it is out of the scope of the protocol and is a basic skill for operating with zebrafish
Step 2.2: The link has been added.

8. In the Protocol, please mention clearly where the microfluidic device was used and the working of the device. Also, please provide the device design and the dimensions as a Supplementary file to help the readers understand better.

> The device is detailed in a publication from one of the authors. We added a reference to this publication in the text and modified Figure 1 to give more details about the system used.

9. Please include all the button clicks, command lines, etc. in the software and on the instruments. Please also ensure that the button clicks are bolded throughout.

> We added more indications in the protocol and bolded the relevant text.

10. Please ensure that the references appear as the following: [Lastname, F.I., LastName, F.I., LastName, F.I. Article Title. Source. Volume (Issue), FirstPage – LastPage (YEAR).] For more than 6 authors, list only the first author then et al. Please include the issue numbers for all references and do not abbreviate the journal names.

> The formatting of all references has been updated.

Reviewers' comments:

Reviewer #1:

Manuscript Summary:
The authors present a semi-automated approach for laser lesioning spinal cord in larval zebrafish. This is an important step forward and the work is presented clearly with some comparisons between mechanical and laser lesions and some observations of glial responses and recovery.

Major Concerns:
I have only one significant concern that they should at least speak to in the paper. The images of the tubulin immuno staining of a lesion site clearly show the completeness of that lesion and they wisely do that staining to speak to the question of bleaching versus a cut. Some of the fluorescence images of lesions in other figures also suggest a complete lesion as the lesion site is black. The concern is that other images of lesion sites, for example the one in figure one, and the one in Fig. 5B, while dimmer in the lesion area show structure, visible after zooming in, with what appear to be fluorescent cells and it seems that spinal cord integrity may be intact. It looks as if these may just be bleaching, even though they obviously can cut the cord in some cases, as in the one for which they show immunostaining. Perhaps they can speak to how reliable a total cut is and is there a way to verify with confidence in the living fish prior to studies of dynamic aspects of regeneration. I am still a bit worried about bleaching versus a cut. It may not matter for many experiments as long as partial cord is cut, but it could be an issue that affects reproducibility.

> We agree with the Reviewer that the images chosen were not representative of a successful lesion. We have replaced them with more typical example of what is to be expected. We are confident that we can induce reproducible lesions, based on the following observations: 14 out of 16 animals that were processed for tubulin immunohistochemistry after laser injury showed a complete transection. We have added this data now to the manuscript.

Moreover, additional qualitative observations support the notion of physical damage. For example, calcium functional imaging demonstrates that the neuronal activity is not propagated anymore between both sides of the lesion, and we observe tissue movements and axons regrowth after laser lesions in a similar way to manual lesions (data not shown). We have added these considerations to the manuscript.

Lastly, we demonstrate in this paper that laser lesions trigger an immune response, which would very unlikely be the case if only photobleaching was happening.

Minor Concerns:
Line 354 they refer to panel 4F in a figure, but there is no 4F panel.

> We thank the review for spotting this mistake and have corrected the wrong panel labelling.

Reviewer #2:
Manuscript Summary:
This paper demonstrates laser induced spinal cord injury in zebrafish larvae. It indicates damage to muscle, neurons, with minimal skin damage. Evident is motoneuron regeneration, axonal regeneration, macrophage infiltration, Ca++ signal recovery (more so rostrally than caudally). It contains software acquisition information for both imaging and UV laser ablation. It is a very strong paper of wide use to the zebrafish community, and possibly other scientists who utilize transparent organisms.

Major Concerns:
Figure 4 B and C. It does appear that the fish has widespread damage and is not confined to the spinal cord. The figure legend states disruption to the "tissue." It's unclear if it is meant to indicate just neural tissue or surrounding somite/skin tissue as well. Many other images offer cleaner examples of laser induced injury without surrounding tissue damage. Since acetylated tubulin is used widely, the extent of damage should be more clearly indicated. Perhaps a comparative brightfield image? Or a reworking of the figure legend.

> We agree with the Reviewer. While some damage to the fixed tissue is to be expected due to the immunolabeling procedure that is not related to the previous laser injury in the living animal, the post-fixation damage in the experiment shown is excessive and distracts from point we are making. We have replaced the images by more representative ones and clarified the legend.

Minor Concerns:
Specify E3 in all areas it is required.

> We now specify where we used fish water or E3 in relevant places in the text.

Specify objective lenses (sections 2 and 3)

> We now specify the objective lens used.

Specify whether scope is inverted or upright? General microscope set up is unclear, seems it would be inverted, but a compound image is shown. Perhaps an image of the actual rig might be informative for others to get a better sense.

> The actual microscope picture is present on figure 1 showing that an upright stand is used. We specify this now in the figure 1 legend.

Line 169-please specify priming media (water, E3, other?)

> Both fish water and E3 can be used. This is now specified in the text.

Line 279-I'm assuming the collected larvae go back into original wells. If so, please state so, it is a nice perk of the system to keep track of different ablation parameters, for example.

> Collected larvae go into a new plate but keep the same well coordinate to ensure tracking them individually, which is indeed a strong benefit of this system.
We have made this clearer in the text and it is now mentioned in the Figure 1 legend.

Line 289- this is more just a comment, seems that E3 used post-lesion (as opposed to switching between E3 and fish water) would be more consistent

> This has been corrected.

Line 298-describe what you mean by unsuccessful lesion. Persistence of fluorophore? or with brightfield? or?

> Unsuccessful lesions are assessed from the remaining fluorescence in the lesion site, apart from the expected residual and homogenous background. We clarified this in the text.

Please state whether PTU is used, and why/why not. Seems like it might be needed for different staged animals?

> In our conditions, PTU was not required. We explicitly state this in line 145.

ROI for laser should be "larger than spinal cord" please provide more anatomical detail, for example, should extend dorsal to skin and ventral to notochord, etc.

> More detail has been given.

Materials: add info for acetylated tubulin

> This is detailed in the Supplemental material

consistent wording: sometimes "section" is used when "transection" might be more appropriate, but it is a little unclear

> We have checked the manuscript to consistently use “transection”, now.

Figure 3: state whether imaging was done immediately after lesion or after some recovery time.

> Imaging was done immediately after lesion. This is now mentioned in the legend.

Figure 4: "complete" transection is a little unclear to this reviewer. Is this to mean in the dorsal-ventral axis, or medial-lateral, or both?

> A complete transection means that on both axes, all the cells have been ablated and axons transected, such that no physical contact remains between the rostral and caudal spinal cord. We specify this in the legend to make it clearer for the reader.

Figure 5: Functional recovery through GCamp6s: this reviewer is a little unclear on what to expect with GCamp6s Fluor intensity in rostral or caudal sections in UNlesioned larvae. This can be clarified in the text. also, I wasn't clear on caudal responsiveness percentage. I think the GCamp Fluor was spontaneous as opposed to evoked, so the term "responsiveness" seemed out of place. Finally, please specify whether animals were still anesthetized when GCamp imaging was done. Were they still in their capillaries?

> We thank the reviewer for highlighting this. We have hopefully clarified all these aspects in the text and figure legend. The term “responsiveness” is indeed unclear and has been replaced by “Connectivity Restoration Index”, which reflects that spinal activity is coordinated along the spial cord. GCaMP fluorescence reveals calcium concentration variations independently of the source of activity, spontaneous or evoked. We tested both and found that the use of spontaneous activity was easier and less prone to bias.
Animals were still anesthetized but not in the capillary. They were mounted in low-melting point agarose for imaging on a separate single point laser scanning confocal microscope. This information has been added at line 355.

Material and Methods

Publication:
Controlled semi-automated lased-induced injuries for studying spinal cord regeneration in zebrafish larvae

Francois El-Daher[1], Jason J. Early[1], Claire E. Richmond[1], Rory Jamieson[1], Thomas Becker[1, 2], Catherina G. Becker[1, 2]

[1] Centre for Discovery Brain Sciences, University of Edinburgh Medical School: Biomedical Sciences, Edinburgh EH16 4SB, UK
[2] Center for Regenerative Therapies at the TU Dresden, Fetscherstraße 105, 01307 Dresden, Germany

---

Animals
All zebrafish lines were kept and raised under standard conditions (Westerfield, 2000) and all experiments were approved by the UK Home Office (project license no.: PP8160052). For experimental analyses, we used up to 5-day-old larvae of either sex of the following available zebrafish lines: Tg(Xla.Tubb:DsRed;mpeg1:GFP)[1,2], Tg(Xla.Tubb:DsRed)[1], Tg(beta-actin:utrophin-mCherry)[3], Tg(Xla.Tubb:GCaMP6s)[3], Tg(mnx1:gfp)[4].

Generation of transgenic zebrafish
The protocol to generate transgenic fish expressing fluorescent reporter follows the work of Higashijima et al.[5] Briefly, cDNA constructs were injected in 1-4 cell stage embryos. Positive embryos were grown to maturity leading to founder animals (F0) mosaic for the fluorescent reporter expression. F0 fish were outcrossed with WT animals to generate heterozygotes offspring (F1). Positive F1 animals were incrossed to produce homozygous F2 fish.

Manual spinal cord injuries
Zebrafish larvae at 3 dpf were anaesthetised in PBS containing 0.02 % aminobenzoic-acid-ethyl methyl-ester (MS222, Sigma), as previously described[6]. Larvae were transferred to an agarose-coated petri dish. Following removal of excess water, the larvae were placed in a lateral position. A 30 G syringe needle was used to make a cut on the dorsal part of the trunk to transect the spinal cord at the level of the 15th myotome, taking care to cut through the spinal cord and to avoid the notochord and major blood vessels. Following injury, larvae were returned to conditioned water and left to develop normally.

Acetylated-tubulin immunohistochemistry
All incubations were performed at room temperature unless stated otherwise. At the time point of interest, larvae were fixed in 4 % PFA-PBS containing 1 % DMSO at 4°C overnight. After washes in PBS, larvae were washed in PBTx (1% Triton X100 in PBS). After permeabilization by incubation in PBS containing 10 µg/ml Proteinase K for 15 min, larvae were washed 2x in PBTx. Then larvae were incubated for 1h in 4% BSA-PBTx (blocking buffer) and incubated with primary antibody (mouse anti-tubulin acetylated antibody, Sigma) diluted

at 1:300 in blocking buffer at 4°C overnight. On the following day, larvae were washed 6 x in PBTx for 20 min each, followed by incubation with secondary antibody (anti-mouse Cy3, Jackson) diluted at 1:300 in blocking buffer at 4°C overnight. The next day, larvae were washed 6 times in PBTx for 30 min each and twice in PBS for 15 min each, before mounting in 1% low-melting point agarose for imaging.

Hb9/EdU staining

EdU staining was performed in Hb9:GFP fish as previously described[7]. Manual and laser lesions were carried out on 3dpf Hb9:GFP larvae as described above. After performing the lesions, larvae were immediately placed in a solution of 50 µm 5-ethynyl-2'-deoxyuridine (EdU; Sigma-Aldrich) and were allowed to develop in this solution.

At 5 dpf (48 hpi) the larvae were culled with an overdose of MS-222 and fixed with 4% paraformaldehyde (PFA) overnight on a rocker. Larvae were washed 3 times with PBSTx (0.2% Triton X-100 in PBS) and placed in methanol at -20°C overnight. Samples were rehydrated in a dilution series from methanol to PBSTx and then washed in PBSTx. The heads of the larvae were then removed with dissection scissors. Larvae were digested using Proteinase K (10 µg/ml in PBSTx) for 45 minutes at room temperature. The EdU Click-iT reaction solution (Roche) was prepared according to manufacturer's instructions and larvae were incubated at room temperature in the dark for 2 hours. All further incubations, including the immunohistochemistry, were carried out in the dark. Larvae were thoroughly washed several times in PBSTx before proceeding to immunohistochemistry.

Anti-GFP staining was performed, as the GFP fluorescence of Hb9:GFP larvae can be low. Anti-GFP staining enhances this fluorescence. Larvae were first blocked in blocking buffer (1% DMSO, 1% goat serum, 1% BSA and 0.7% Triton X-100) for 2 h. Larvae were incubated with the primary antibody (chicken anti-GFP, 1:300 dilution; Abcam Cambridge) overnight at 4°C, and then washed thoroughly in PBSTx. A further overnight incubation in secondary antibody was done at 4°C. The larvae were finally washed in PBSTx, mounted in glycerol, and imaged.

Imaging

For calcium imaging, Tg(Xla.Tubb:GCaMP6s) larvae lesioned following the laser lesion protocol were mounted alive at different time points after injury on a glass coverslip embedded in 2% low melting point agarose and imaged using a spinning-disk confocal microscope (3i- Intelligent Imaging Solutions, Denver) equipped with a 20x NA 1.0 LWD water dipping objective lens and two EMCCD cameras (Orca, Hamamatsu). The same equipment was used for living imaging on Tg(NBT:dsRed;mpeg1:GFP).

For imaging of live Tg(Beta-actin:utrophin-mCh) larvae, we used a Zeiss LSM880 confocal microscope equipped with an Airyscan detector and a 20x NA 1.0 LWD water dipping objective lens. The larvae were mounted laterally in 1% low melting point agarose on a microscope slide and imaged approximately 1 hr after injury.

To obtain pictures of the skin, larvae were pinned through the notochord to a Sylgard (Sylgard 184, Dow) platform using thin (1mm diameter) tungsten wire pins. Images were taken on a Leica stereo microscope.

For imaging of fixed larvae, we used either the Zeiss LSM880 confocal (anti-acetylated tubulin staining) or a Zeiss ApoTome microscope with 10x NA 0.45 objective lens (Edu/anti-GFP staining).

Image processing and analysis

For quantification of calcium imaging data, all time-lapse images were first motion-corrected in Fiji using the plugin Moco (https://github.com/NTCColumbia/moco). Fluorescent signal was then measured over time using Fiji by drawing regions of interest (ROI) by hand in the desired locations. Caudal responsiveness estimated calculated as the ratio of the amplitude of the fluorescence peaks in the caudal ROI by the amplitude in the rostral ROI.

Long-term imaging data were registered for 3D motion in Fiji using the plugin correct 3D drift (https://imagej.net/plugins/correct-3d-drift).

The quantification of macrophage accumulation at 6 hpi was done by counting mpeg1:GFP+ cells in a ROI at the injury site

References

1. Peri, F. & Nusslein-Volhard, C. Live imaging of neuronal degradation by microglia reveals a role for v0-ATPase a1 in phagosomal fusion in vivo. *Cell* 133, 916–927 (2008).
2. Ellett, F., Pase, L., Hayman, J. W., Andrianopoulos, A. & Lieschke, G. J. mpeg1 promoter transgenes direct macrophage-lineage expression in zebrafish. *Blood* 117, e49–e56 (2011).
3. Established by David Greenhald, University of Edinburgh.
4. Flanagan-Steet, H., Fox, M.A., Meyer, D., and Sanes, J.R. Neuromuscular synapses can form in vivo by incorporation of initially aneural postsynaptic specializations. *Development* 132(20):4471-4481. (2005)
5. Higashijima, S., Okamoto, H., Ueno, N., Hotta, Y. & Eguchi, G.1997. High-frequency generation of transgenic zebrafishwhich reliably express GFP in whole muscles or the wholebody by using promoters of zebrafish origin. Dev. Biol. 192,289 –299
6. Wehner, D. et al. Wnt signaling controls pro-regenerative Collagen XII in functional spinal cord regeneration in zebrafish. *Nature Communication.* **8** (126), 1–16 (2017).
7. Ohnmacht, J. et al. Spinal motor neurons are regenerated after mechanical lesion and genetic ablation in larval zebrafish. *Development*. **143** (9),1464–74 (2016).